Urban heat island behaviors in dryland regions

Environmental Research Communications

LETTER

Urban heat island behaviors in dryland regions

John M Dialesandro[1,4], Stephen M Wheeler[2] and Yaser Abunnasr[3]

[1] University of California Davis, Geography Graduate Group, Davis, CA, 95616-5270, United States of America
[2] University of California - Davis, Department of Environmental Design, Davis, CA, 95616, United States of America
[3] American University of Beirut, Department of Landscape Design and Ecosystem Management Beirut, Lebannon
[4] Author to whom any correspondence should be addressed.

E-mail: jdiales@ucdavis.edu, smwheeler@ucdavis.edu and ya20@aub.edu.lb

Keywords: urban heat islands, urban forest, land surface temperature, vegetative cooling, dryland cities

OPEN ACCESS

RECEIVED
24 May 2019

REVISED
24 July 2019

ACCEPTED FOR PUBLICATION
1 August 2019

PUBLISHED
22 August 2019

Abstract

Urban heat island (UHI) characteristics and mitigation strategies for dryland cities differ from those for wetter urban regions. Whereas the latter typically see daytime surface UHIs, the rapid heating and cooling of deserts surrounding arid cities often produces daytime 'urban cool islands' and nighttime UHIs. Degrees of aridness, extent of vegetation, elevation, latitude, humidity, topography, and typical building types are likely to influence dryland UHI dynamics. This study analyzes variations in thermal effects at multiple scales for 10 dryland urban regions representing varied geographies worldwide with an aim to establish a broader understanding of the spectrum of UHI patterns in dryland cities. We used GIS to assemble daytime and nighttime satellite imagery, determined land surface temperature and vegetation at a 30-meter scale, and analyzed typical neighborhood-scale examples of six land cover types in each region. The 10 regions showed large variation in thermal effects. We found a strong daytime surface UHI in only one. Nighttime heat islands were more pronounced. However, all regions showed strong small-scale variation in temperature, averaging a 12.3 °C difference between mean top-quintile and bottom-quintile surface temperatures. Samples of urban forest landscapes cooled daytime temperatures an average of 5.6 °C compared to metro averages. Irrigated lawn and multistory building land cover samples also had a substantial cooling effect. Xeriscaped landscapes amplified daytime heating. Our results indicate that UHIs for dryland cities are unlikely to be reduced by xeriscape strategies, but that shade-maximizing urban forestry and built form hold promise to reduce heat islands.

1. Introduction

Urban heat islands (UHIs) often form in temperate climates as buildings and paved surfaces absorb and slowly release solar radiation during the daily cycle, making cities warmer than surrounding vegetated rural landscapes (e.g. Schatz and Kucharik). However, an emerging literature indicates that UHI dynamics are more complicated for dryland cities, a category that includes arid, semi-arid, and Mediterranean climates (Connors *et al* 2013, Nassar *et al* 2016). While there are a multitude of studies that focus on temperate regions there are less that focus on dryland regions and even fewer that do a global comparison.

This study analyzes how urban heat island effects vary across 10 dryland urban regions representing a range of geographical environments worldwide. We determine differences between day and night mean urban and rural temperatures derived from satellite imagery, consider variation of temperatures at a detailed (30-meter) scale within the urban area, and correlate land surface temperature with vegetation. To assess the impact that certain built landscape types have on surface temperatures, we analyze representative samples of six land covers in each region—urban forest, irrigated turf and tree, xeriscape, hardscape, urban multistory, and undeveloped—and compare their temperature with the urban and rural mean. These methods, described further below, allow us to draw conclusions related to ways that urban temperatures, vegetation, and built form vary across a

range of dryland urban regions, and potentially how urban heating and UHIs can be mitigated through landscape planning.

Urban heat islands are the net result of several physical processes that include radiative, thermal, aerodynamics and moisture built form, materials, and vegetation. These processes include the absorption of sunlight and re-radiation of heat by dark surfaces such as pavements and roofs; the reflectance of sunlight by light-colored materials; shading produced by trees and buildings; and evapotranspiration from plants which cools the surrounding air. The configuration of land covers within the urban environment influences these dynamics (Middel *et al* 2014, Song and Wang 2015).

UHIs can be identified through satellite land surface temperature measurements or by onsite measurements at 2-m pedestrian or tree-canopy level. They can also be modeled with computer software. Starting in the 1970s researchers showed that dark surfaces tend to produce higher air and surface temperatures than the urban mean (Oke 1973), while green spaces tend to produce lower temperatures (Spronken-Smith and Oke 1998, Onishi *et al* , Chow *et al* 2011). Temperature differences between natural and anthropogenic land covers can vary by up to 5 °C for adjacent sites and up to 9 °C between urban core and rural areas (Imoff *et al* 2010).

Although two-meter air temperatures may be most relevant for human comfort, surface temperatures are more frequently studied owing to the easy availability and comprehensiveness of satellite data. Surface temperatures tend to show heating more strongly than air temperatures. They generally correlate with air temperatures but do not directly correspond due to atmospheric mixing and materials properties as well as technical measurement issues (Zhou *et al* 2019).

Within the past decade several large-scale studies have documented a daytime 'urban cool island' effect for many dryland cities as surrounding landscapes with sparse xeric vegetation, grasses, and dry soils warm more rapidly than urban surfaces (Imhoff *et al* 2010, Peng *et al* 2014, Chakraborty and Lee 2019). Surrounding deserts then cool more rapidly at night than urban pavement and rooftops, leading to nighttime UHIs. However, the case study literature suggests variability in this effect. Degrees of aridness, extent of vegetation, elevation, latitude, humidity, and typical building types are likely to influence dryland urban heat island behaviors (Zhou *et al* 2014, Heinl *et al* , He *et al*).

Research shows the importance of vegetated spaces such as lawns, parks, street trees, and green roofs in reducing dryland UHIs through evapotranspiration and shade (Bowler *et al* 2010, Rchid 2012, Wang *et al* 2016). However, conventional turf-and-tree landscapes require consistent irrigation. Xeric landscapes using native and/or drought tolerant species use less water, but are likely to have less cooling effect since xeric species tend to have thin foliage and minimize evapotranspiration (Connors *et al* 2013).

High-density urban parcels with buildings that create shade can reduce local heating (Emmanuel and Fernando 2007, Norton *et al* 2015, Nassar *et al* 2016, 2017). Street width, building height, and tree canopy level all affect this dynamic (Coseo and Larsen 2014). Urban heat islands in most climates are prominent at night because street canyons tend to trap heat in addition to urban materials often experiencing a slower nighttime cooling rate than natural surfaces (Connors *et al* 2013).

2. Methodology

We investigated UHI behavior for dryland cities at three scales: the metropolitan region, the neighborhood, and the 30-meter pixel scale available from satellite imagery. We chose a global convenience sample of 10 large dryland urban regions selected to reflect a diversity of dryness, seasonality, urban growth, elevation, and built form. These regions include hyper-arid, arid, Mediterranean, monsoonal, and dry high-altitude climates, but all have an overall water deficit throughout the year and long annual periods with no rain. Eight are located in the northern hemisphere, and two in the southern. We defined urban boundaries for each metropolitan area using city boundaries from Open Street Map (https://www.openstreetmap.org). Surrounding each region we established a 20 kilometer-wide rural buffer for comparison purposes as can be seen in figure 3. To enhance uniformity, we removed water bodies, as well as areas within 5 km of water bodies for all regions as it has been found that marine influences can vary influence in degree of extent inland (Efthymiadis and Jones), Elevations exceeding 500 feet of the regional mean were also masked out.

We acquired Landsat 8 OLI and ASTER data (30-meter resolution) for daytime and nighttime hot-season dates, and derived land surface temperature (LST) from these sources (table 1). Google Earth Engine, and QGIS were utilized to acquire and process the imagery to Land surface temperature We sampled daytime data near 11 AM local time, and nighttime data near 10 PM. Areas that required two scenes to cover metro areas were mosaiced if scenes were captured on same day (i.e. same path for Landsat), but scenes from different Landsat rows were not mosaiced if they were in different rows due to the temporal differences in scene capture time. For regions with monsoonal influences, we chose dates close to the end of the dry season. At the metropolitan scale

Table 1. Dates and source of thermal imagery.

City	Day	Night	Day Image	Night Image
Cairo	07/29/2017	08/08/2015	Landsat 8 OLI	Landsat 8 OLI
Delhi	05/15/2017	08/04/2017	Landsat 8 OLI	ASTER
Dubai	07/28/2016	06/30/2017	Landsat 8 OLI	ASTER
La Paz	11/24/2017	07/07/2018	Landsat 8 OLI	ASTER
Lima	05/10/2017	05/07/2018	Landsat 8 OLI	ASTER
Los Angeles	08/09/2016	07/08/2016	Landsat 8 OLI	Landsat 8 OLI
Madrid	07/17/2017	06/25/2916	Landsat 8 OLI	Landsat 8 OLI
Mexico City	05/28/2016	05/17/2017	Landsat 8 OLI	Landsat 8 OLI
Tehran	06/23/2017	06/09/2016	Landsat 8 OLI	ASTER
Phoenix	08/15/2017	08/12/2016	Landsat 8 OLI	Landsat 8 OLI

we extracted the mean temperatures of the entire region, mean temperatures of upper and lower quintiles of 30-meter pixels, and mean temperature of the surrounding rural areas.

We employed a broadly used method that from the Landsat Handbook for LST retrieval. In this method, only TOA (Top of Atmosphere) radiance and NDVI (Normalized Difference Vegetation Index) are required. According to the handbook, the TOA radiance of thermal infrared band is converted to TOA (or at-sensor) brightness temperature based on the formula (equation (1)) (Chander *et al* 2009, Jimenez- Munoz *et al* 2014):

$$\text{Tsensor} = \text{K1}/\ \ln\left(\text{K2}/(\text{L}\lambda + 1)\right) \tag{1}$$

where Tsensor is the at-sensor brightness temperature in Kelvin (K) and L is the TOA radiance in $\text{W}/\text{m}_2\text{Srum}$. For Landsat-8 TIRS, K1 is 774.89 W m^{-2} Srμm) and K2 is 1321.08 K for band 10 (USGS, n.d.).

The following equation (equation (2)) calculates the LST based on the brightness temperature obtain previously (Artis and Carnahan 1982).

$$\text{LST} = \text{Tsensor}/((1 + \lambda * \text{Tsensor}/\alpha) * \ln(\varepsilon)) \tag{2}$$

where LST is the land surface temperature in Kelvin (K), λ is the wavelength in meters and $= 1.438 \times 10^{-2}$ mK. represents the surface emissivity which differs from various land cover types (Shen *et al* 2016). For ε, water (NDVI < 0) was assigned a value of 0.9925, urban impervious areas and bare soil ($0 = <\text{NDVI} < 0.15$) were assigned a value of 0.923, and vegetation (NDVI > 0.727) was assigned a value of 0.986. Otherwise, there was a modeling relationship with the NDVI values through the following equation:

$$\varepsilon = 1.0094 + 0.047 * \ln(\text{NDVI}) \tag{3}$$

For ASTER imagery we used the same conversion to surface brightness temperature as Landsat. The imagery was then corrected to surface temperature using band 13 (10.6 micrometers) because of the thermal bands available for ASTER, band 13 lined up closest in spectral wavelength designation as that of Landsat 8 OLI Band 10.

$$\text{LST} = \text{band13}/(1.0094 + 10.6 * \text{band 13})/ \\ 14388 * \ln(\text{emissivity})) \tag{4}$$

To analyze neighborhood-scale effects, we used Google Earth Engine to visually identify representative samples exceeding one square kilometer in size of six different land cover types (see figure 1). We elected to use this domain expert approach to ensure near 100% accuracy, rather than employing a machine learning classification algorithm such as the World Urban Database Access Portal Tools (Verdonck *et al* 2019) to quickly classify such areas with moderate accuracy (70%–85%). Our approach was similar to that used by the HERCULES model for classifying urban patches (Cadenasso *et al* 2007). The selected land covers were:

- Urban Multistory: urban neighborhoods with closely spaced buildings of three stories or more, able to cast substantial amounts of shade
- Irrigated Turf and Tree: large areas of turfgrass with scattered trees (less than 25% tree canopy), including parks, golf courses, playing fields, and residential neighborhoods with sizable yards
- Xeriscape: developed areas with sparse, native and/or drought-tolerant vegetation, typically also including substantial amounts of bare dirt
- Hardscape: low-rise urban environments with extensive impermeable surfaces such as streets, parking lots, and rooftops

Figure 1. Six neighborhood scale land cover types.

- Urban forest: areas with dense tree canopies (native and non-native) (>70%), typically found along waterways or in densely vegetated parks
- Unbuilt: undeveloped land areas within or external to the urban area

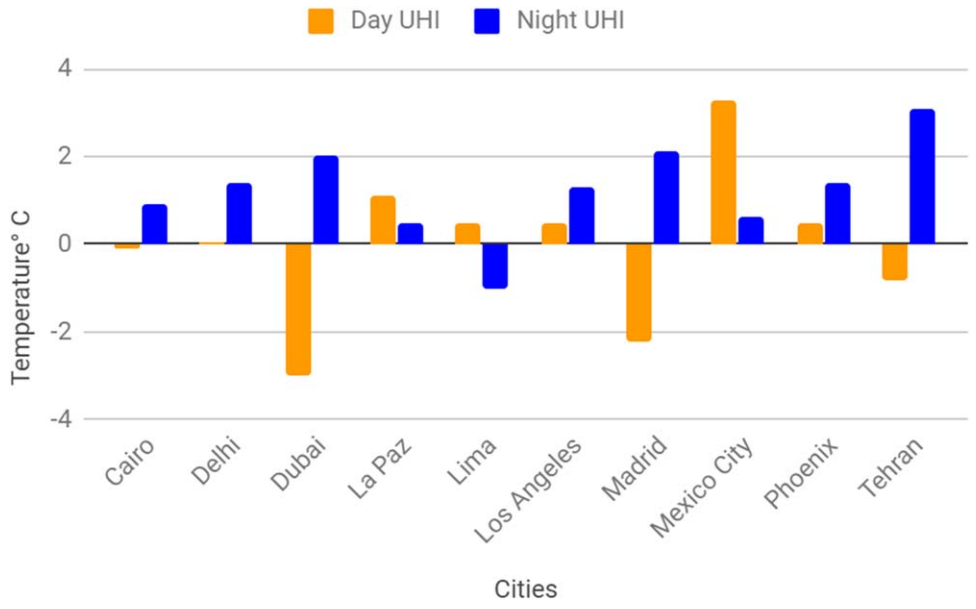

Figure 2. Daytime and nighttime surface UHI magnitudes for 10 dryland cities.

To assess spillover temperature effects, we also formed one-kilometer buffers around these built landscape samples and analyzed average temperature differences between the six land cover types, surrounding buffer areas, and the urban mean.

3. Results

3.1. Metropolitan Scale

At the metropolitan scale, we found that only one of the ten regions (Mexico City) had an average daytime surface temperature substantially higher (>2 °C) than the surrounding rural. mean, in the traditional urban heat island pattern. Two of the regions (Dubai and Madrid) showed substantial daytime urban cool island effects (temperatures >2 °C below the rural mean). Most of the regions had average temperatures close to the rural mean, showing little overall daytime UHI effect (See figure 2). At night three of the 10 regions had substantial (>2 °C) UHI effects (Dubai, Tehran, and Madrid), while five others had lesser effects of around 1 °C. Delhi exhibited no urban heat island pattern (<0.1 °C). Figure 3 presents a comparison of daytime and nighttime urban heat island intensities. In all cases the standard deviation and range of temperatures were lower at night for both urban and rural areas. We assume that this is a result of rapid daytime heating of certain landscape surfaces, and more gradual diffusion of thermal energy at night (Spronken-Smith and Oke 1998).

Although some regions showed little overall surface UHI, particular locations within them experienced strong heating and cooling during both day and night (Tables 3 and 4). The hottest quintile of 30 meter pixel surface temperatures was on average 5.2 °C warmer during daytimes than the mean for rural lands. Meanwhile, the coolest quintile of daytime surface temperatures was an average of 4 °C cooler than the mean of non-urban land (see tables 1 and 2). The mean difference across these 10 regions between the hottest and coolest quintiles of surface pixel temperature was 12.3 °C.

Many regions showed weak 30-meter correlations between vegetation and lower surface temperatures. However, the only statistically significant relationship was for rural areas near Cairo during the daytime. This correlation is likely the product of dense agricultural development of the Nile River Delta.

3.2. Neighborhood scale

At the neighborhood scale, different types of land cover appear to vary strongly in surface temperature compared to the mean for these regions (Figure 4). Our sample of urban forest land cover produced the greatest daytime temperature reduction, an average decrease of 5.6 °C. In Phoenix, Arizona, the urban forest sample was 16.5 °C cooler than the metro mean during daytime (Table 5). A surrounding one-kilometer buffer area around each urban forest sample also experienced spillover cooling effects, with an average temperature reduction of 1.7 °C. These cooling effects of urban forest land covers relative to the regional mean disappeared at night (Table 6).

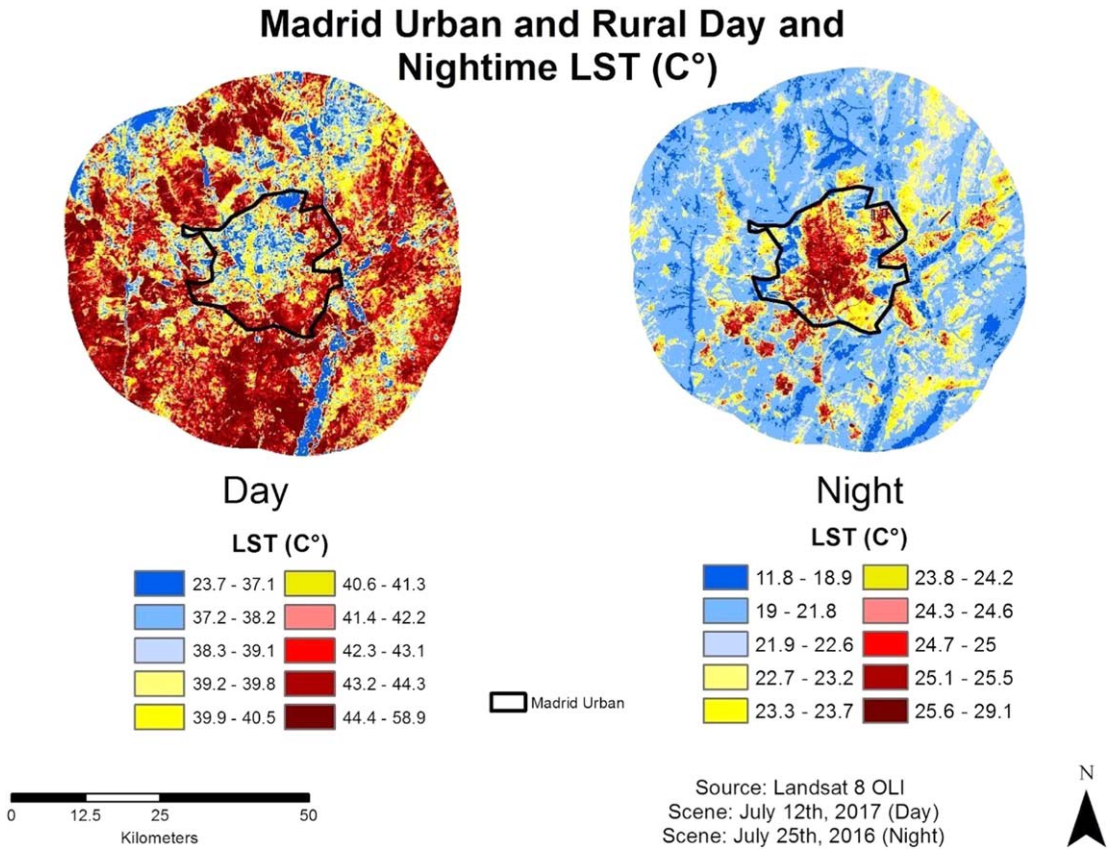

Figure 3. Sample daytime and nighttime urban heat island maps (Madrid). Caption: Madrid Urban with 20 km buffer surrounding urban metro boundary. Thinly vegetated dry land outside Madrid warms more rapidly during the day than urban landscapes. At night the city retains heat while rural areas cool.

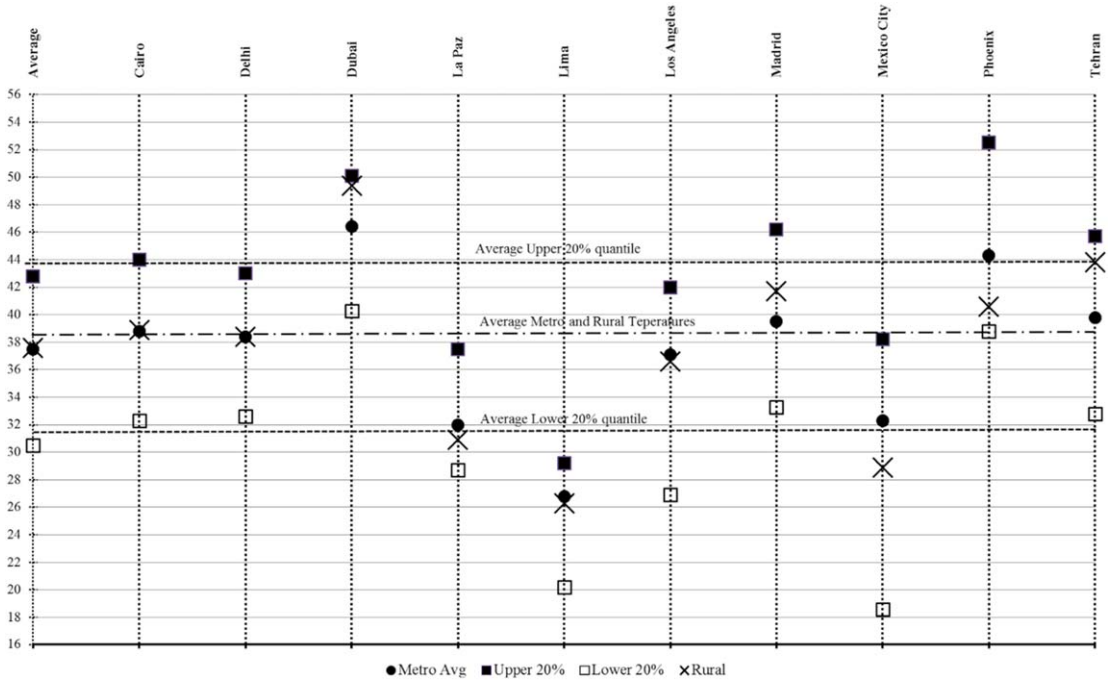

Figure 4. Daytime temperature variation by sample neighborhood-scale land cover for 10 regions Caption: Different sample neighborhood-scale land cover types have large daytime temperature differences (°C). Degree of variation differs by region. Urban forests were generally coolest, and unbuilt and hardscaped land covers the hottest.

Table 2. Average top and bottom quintile daytime temperatures compared with metro and rural means (°C).

Cities	Rural Mean (°C)	Metro Mean (°C)	Upper 20% of 30 m pixels (°C)	Lower 20% of 30 m pixels (°C)	Difference (°C)
Cairo	38.9	38.8	44.0	32.3	11.7
Delhi	38.4	38.4	43.0	32.6	10.4
Dubai	49.4	46.4	50.1	40.3	9.8
La Paz	30.9	32.0	37.5	28.7	8.8
Lima	26.3	26.8	29.2	20.2	9.0
Los Angeles	36.6	37.1	42.0	26.9	15.1
Madrid	41.7	39.5	46.2	33.3	12.9
Mexico City	28.9	32.3	38.2	18.6	19.6
Tehran	43.8	39.8	45.7	32.8	12.9
Phoenix	40.6	44.3	52.5	38.8	13.7
Average	37.6	37.5	42.8	30.5	12.3

Table 3. Average top and bottom quintile night temperatures compared with metro and rural means.

Cities	Rural Mean (°C)	Metro Mean (°C)	Upper 20% Lower of 30 m pixels(°C)	20% of pixels 30 m pixels(°C)	Difference (°C)
Cairo	25.6	26.5	28.3	24.8	3.5
Delhi	24.2	25.6	28.4	22.7	5.7
Dubai	24.2	26.2	29.6	23.1	6.5
La Paz	2.5	3.0	4.5	−3.2	7.7
Lima	15.6	14.6	17.2	12.8	4.4
Los Angeles	16.4	17.7	21.5	14.7	6.8
Madrid	21.3	23.4	26.4	17.7	8.7
Mexico City	16.3	16.9	20.1	10.8	9.3
Phoenix	24.4	25.8	29.0	22.7	6.3
Tehran	19.5	22.6	24.8	19.8	5.0
Average	19.0	20.2	23.0	16.6	6.4

Our irrigated turf and tree sample land covers also produced daytime cooling effects in all cities, an average temperature reduction of 2.0 °C from the mean. The spillover cooling impact was weaker than for urban forests, and nighttime temperature differences from the urban mean were negligible.

Urban multistory land cover samples were cooler than the daytime mean in 7 of the 10 metro regions, with an average temperature reduction of 1.0 °C (Table 7). The strongest cooling effects were found in Dubai, Cairo, and Lima. Cooling effects disappeared for multistory samples in most regions at night. For Dubai and La Paz, urban multistory samples had substantially warmer nighttime temperatures than the urban average (Table 8). However, these may have risen for contextual reasons: Dubai's downtown is relatively near the Persian Gulf, which likely moderates temperatures, and La Paz is at very high elevation, which leads to very rapid cooling of unbuilt areas and a low mean regional nighttime temperature.

Xeriscape land cover samples were generally warmer than the average daytime metro temperature—an average of 1.8 °C. In five of the 10 regions, the sample of this land cover type was more than 2.4 °C above the metro mean. However, there were few spillover effects to surrounding areas. At night xeriscape samples showed no difference from regional average temperatures. Samples of unbuilt areas within the metro regions were also typically warmer than the mean for these 10 dryland urban areas—an average of 1.4 °C. At night these samples were cooler than the metro mean—an average of 0.5 °C. These findings are to be expected, as these samples mirror rural arid landscapes with rapid daytime heating and nighttime cooling. We found the unbuilt sample for Mexico City to be much cooler than in the other regions during the daytime, which may be due to more extensive vegetation or topography.

4. Discussion

Our analysis confirms that dryland urban regions have substantially different surface UHI characteristics than the literature has shown for wetter, temperate regions. Daytime urban cool islands are likely due to the rapid heating characteristics of surrounding arid terrain. But this phenomenon shows high variability. Modest nighttime UHIs usually occur since rural arid landscapes cool more rapidly than urban ones. The large variation in metro-scale thermal effects between these 10 dryland regions can most likely be explained by factors such as

Table 4. 10 Dryland urban regions compared.

Urban region	Climate (koppen)	Precip. (mm)	Elev (m)	Pop. (mil.)	Pop. Density (per./km^2)	Average hottest month humidity	Average daytime temp. diff. urban/rural	Average nighttime temp. diff. urban/rural
Cairo	Hot Desert (BWh)	24.7	25	20.4	38 636	58%	0.1 °C	0.9 °C
Delhi	Warm Steppe (BSh)	800	230	26.5	17 857	33%	0.0	1.4
Dubai	Hot Desert (BWh)	201	10	5.6	1,363	56%	−3.0	2.0
La Paz	Subtropical Highland (CWc)	564	3,640	2.7	5,720	43%	1.1	0.5
Lima	Mild Desert (BWn)	16	0–1,550	12.1	15 125	85%	0.5	−1.0
Los Angeles	Mediterranean (Csb)	384	80	18.7	14,363	73%	0.5	1.3
Madrid	Mediterranean (Csa)	436	730	6.7	11 093	35%	−2.2	2.1
Mexico City	Subtropical Highland (Cwb)	820	2,450	20.9	14 074	43%	3.3	0.6
Phoenix	Hot Desert (BWH)	200	300	4.7	3,500	32%	0.5	1.4
Tehran	Cool Semiarid (BSK)	220	1,650	8.7	11 918	31%	−0.8	3.1

Gray = Temperature differences over 2 °C.

Table 5. Daytime urban forest covers surface temperature compared to metro mean of entire area.

Region	Metro mean temp. (°C)	Urban forest versus Mean of metro area (°C)	<1 km from veg. versus mean of metro area (°C)
Cairo	38.8	−5.5	−0.6
Delhi	38.4	−1.8	−2.0
Dubai	46.4	−5.2	0
La Paz	32.0	−3.6	−1.3
Lima	26.8	−2.4	−1.9
Los Angeles	37.1	−4.2	−0.9
Madrid	39.5	−6.0	−0.2
Mexico City	32.3	−3.6	+0.5
Phoenix	44.3	−16.5	−8.7
Tehran	39.8	−7.0	−2.2
AVERAGE	37.5	−5.6	−1.7

Caption: Urban forests are >2 °C cooler (dark gray) than the urban average for 9 of 10 dryland regions studied, with cooling extending 1 km beyond borders of vegetated space in some cities.

Table 6. Nighttime urban forest temperature compared to metro mean.

Region	Metro mean temp. (°C)	Urban forest versus mean of metro area (°C)	< 1 km from veg. versus mean of metro area (°C)
Cairo	26.5	−0.8	−0.5
Delhi	25.6	−0.6	0.5
Dubai	26.2	−0.7	−1.9
La Paz	3.0	1.0	0.8
Lima	14.6	0.1	0.1
Los Angeles	17.7	−0.7	0.8
Madrid	23.4	1.4	1.5
Mexico City	16.9	1.4	1.8
Phoenix	25.8	−0.1	−0.6
Tehran	22.6	0.2	0.1
AVERAGE	20.2	0.1	0.3

Table 7. Temperatures by land surface type within dryland urban regions (Daytime).

Region	Metro mean temp. (°C)	Urban Forest versus mean (°C)	Irrigated turf and tree versus mean (°C)	Urban multistory versus mean (°C)	Hardscape versus mean (°C)	Xeriscape/dirt versus mean (°C)	Unbuilt versus mean (°C)	Rural (°C)
Cairo	38.8	−5.5	−3.3	−3.0	1.4	−0.1	0	38.9
Delhi	38.4	−1.8	−2.4	−0.6	2.2	0.2	0.8	38.4
Dubai	46.4	−5.2	−3.6	−4.3	3.0	0.4	2.0	49.4
La Paz	32	−3.6	4.2	−0.4	1.4	4.2	0.5	30.9
Lima	26.8	−2.4	−2.9	−2.3	−0.2	−0.3	1.3	26.3
L.A.	37.1	−4.2	−3.6	−0.5	−2.1	2.4	0.3	36.6
Madrid	39.5	−6.0	−3.4	0.7	−0.2	2.7	2.6	41.7
Mexico City	32.3	−3.6	−1.9	−0.4	0.6	2.9	−4.3	28.9
Phoenix	44.3	−16.5	−0.5	2.9	1.5	2.9	5.0	43.8
Tehran	39.8	−7.0	−4.9	−1.9	2.4	1.6	5.6	40.6
AVERAGE	37.5	−5.6	−2.2	−1.0	1.0	1.8	1.4	

Caption: Urban forests, irrigated turf and tree landscapes, and some multistory built landscapes have more than 2 °C cooler surface temperatures (light gray) than the mean during daytime for the sampled land covers. Hardscaped, xeriscaped, and unbuilt landscape surface temperatures are often substantially hotter (dark gray) than the mean.

Table 8. Temperatures by Land Surface Type within Dryland Urban Regions (Nighttime).

Region	Metro mean temp. (°C)	Urban Forest versus mean (°C)	Irrigated turf and tree versus mean (°C)	Urban multistory versus mean (°C)	Hardscape versus mean (°C)	Xeriscape/dirt versus mean (°C)	Unbuilt versus Mean (°C)	Rural (°C)
Cairo	26.5	−0.8	0.5	1.2	1.4	0.3	−0.2	25.6
Delhi	25.6	−0.6	0.5	2.1	2.2	2.0	−1.1	24.2
Dubai	26.2	−0.7	−0.2	3.5	3.0	−0.3	−2.2	24.2
La Paz	3.0	1.0	−0.1	4.0	1.4	−0.6	3.8	2.5
Lima	14.6	0.1	−0.2	0	−0.2	−0.3	−0.1	15.6
Los Angeles	17.7	−0.7	−0.4	0.8	−2.1	−0.3	−0.6	16.4
Madrid	23.4	1.4	−1.5	1.5	−0.2	−0.4	−3.4	21.3
Mexico City	16.9	1.4	0.7	1.1	0.6	0.8	0.1	16.3
Phoenix	25.8	−0.1	−0.1	−1.8	1.5	−0.8	1.0	24.4
Tehran	22.6	0.2	1.2	−0.4	2.4	1.4	−2.7	19.5
AVERAGE	20.2	0.1	0.0	1.2	1.0	0.2	−0.5	

Caption: Differences are not as pronounced at night. In some regions urban buildings and pavement retain substantial surface heat at night (dark gray). Although frequently hotter during the day in arid regions, unbuilt lands are often cooler at night (light gray) than the regional mean temperature.

degree of aridity, extent of vegetation, elevation, humidity, latitude, topography, and typical building types. However, interactions between these factors are likely complex and a large sample would be required to statistically tease out individual variables responsible for such differences, if that in fact could be done. However, even though surface UHIs may not exist for dryland urban regions or may be mild, our analysis shows strong local variation in temperature at the 30-meter scale. This variation is likely due to dark surface materials such as asphalt absorbing solar radiation, light colored surfaces reflecting solar energy, the production of shade by structures, or vegetative cooling. These variations will affect human health and comfort, building cooling loads, and social equity considerations.

The dryland metro areas studied here do not show strong correlations between vegetation and temperature. However, overall amounts of vegetation (especially tree canopy) are low in most of these regions, and it is possible that with higher levels of vegetation greater correlations would be found. When we examined sample neighborhood-scale patches of urban forest, we found large cooling effects. One implication is that ambitious regional urban forestry programs might indeed help cool metro areas. However, such programs would need to take water use for irrigation into account. Potentially, low-water tree species could be found that would yield significant cooling when planted citywide. More investigation into low-water, shade-producing vegetation as well as optimal configuration of green spaces for cooling would be desirable.

The sample irrigated turf and tree landscapes we examined had somewhat smaller but still sizable reductions in daytime surface temperature compared to metro means. Use of this landscape strategy would need to be balanced with water consumption. Turfgrass landscapes and water-intensive broadleaf trees are also known to increase local evapotranspiration and humidity, which can cool local landscapes but also traps heat at night.

Xeriscaped landscapes showed little ability to cool urban regions, and the samples we examined were in fact hotter than the daytime metro mean in most regions. Although these landscapes may be desirable for other reasons such as habitat, aesthetic value, and water conservation, they will probably not be able to help reduce urban heat islands.

Shade-producing built form shows potential to reduce daytime urban heating while improving micro-scale human comfort by providing shaded walkways, sidewalks, and courtyards. The samples of this land cover that we examined were 1 °C cooler than metro means, even though their building types and surface materials were usually conventional in nature. Architects, urban designers, and engineers seeking to maximize the shade cast by structures as well as light-colored roof and paving materials might be able to achieve even stronger daytime cooling effects from urban multistory development.

Our study has limitations that should be mentioned. The spatial resolution of Landsat and ASTER thermal imagery is still relatively coarse, yielding 900 m^2 pixels. Unfortunately, higher spatial resolution thermal imagery is not available. Also, although we attempted to remove noise in the data caused by water bodies, proximity to coasts, and elevation changes, we were not able to do this completely. Even removing a 5 km buffer next to shorelines from analysis in places such as Dubai, Lima, and Los Angeles, urban temperatures were undoubtedly affected to some extent by maritime influences.

Within the neighborhood-scale analysis some challenges arose with consistencies between on-the-ground practices across the ten metro regions. Xeriscape landscape design, for example, is not an active or standardized practice in many of these cities. For those lacking good examples, we chose neighborhoods with a mix of low-water vegetation and bare soil that seemed likely to be closest in performance to xeriscape. The La Paz and Lima regions are lacking in urban forests, and for the urban forest analysis we by necessity chose vegetated riparian canyons on the urban periphery. Shade-producing multistory built form is more common in Mediterranean cities, where narrow streets, arcades, courtyards, and related urban form elements have been used for millennia to enhance thermal comfort. Multistory buildings in Phoenix, by contrast, tend to stand alone among wider streets and extensive surface parking, and so are unlikely to produce the same cooling effect.

5. Conclusion

In the era of anthropogenic climate change, keeping cities cool is a growing priority for human health, energy conservation, and greenhouse gas mitigation reasons. Dryland urban regions face different challenges than cities in wetter climates. This study confirms the absence of daytime urban heat islands for many dryland cities, and, conversely, their presence at night. It also highlights the importance of considering building-scale and neighborhood-scale temperature variations—and reducing temperatures at these scales—whether or not regional UHIs exist. Our findings suggest limited correlations between vegetation and cooling for dryland cities at the metropolitan scale, but stronger correlations at the neighborhood scale. The samples of urban multistory landscapes we analyzed also showed the potential of this landscape type to assist in urban cooling. Xeriscape land covers do not appear to have substantial cooling benefit, although they may be desirable for other reasons. A main takeaway is that land covers mixing drought tolerant urban forestry and shade-maximizing built form may help cool dryland cities sustainably, given water limitation.

ORCID iDs

John M Dialesandro https://orcid.org/0000-0002-9578-7998

References

Artis D A and Carnahan W H 1982 Survey of emissivity variability in thermography of urban areas *Remote Sens. Environ.* **12** 313–29
Bowler D E, Buyung-Ali L, Knight T M and Pullin A S 2010 Urban greening to cool towns and cities: a systematic review of the empirical evidence *Landscape and Urban Planning* **97** 147–55
Cadenasso M L, Pickett S T A and Schwarz K 2007 Spatial heterogeneity in urban ecosystems: reconceptualizing land cover and a framework for classification *Front Ecol. Environ.* **5** 80–8
Chakraborty T and Lee X 2019 A simplified urban-extent algorithm to characterize surface urban heat islands on a global scale and examine vegetation control on their spatiotemporal variability *Int. J. Appl. Earth Obs. Geoinf.* **74** 269–80
Chander G, Markham B L and Helder D L 2009 Summary of current radiometric calibration coeffecients for Landsat MSS, TM, ETM+, and EO-1 ALI sensors *Remote Sens. Environ.* **113** 893–903
Chow W T, Pope R L, Martin C A and Brazel A J 2011 Observing and modeling the nocturnal park cool island of an arid city: horizontal and vertical impacts *Theoretical and Applied Climatology* **103** 197–211
Connors J P, Galletti C S and Chow W T 2013 Landscape configuration and urban heat island effects: assessing the relationship between landscape characteristics and land surface temperature in Phoenix, Arizona *Landscape Ecology* **28** 271–83
Coseo P and Larsen L 2014 How factors of land use/land cover, building configuration, and adjacent heat sources and sinks explain Urban Heat Islands in Chicago *Landscape and Urban Planning* **125** 117–29
Efthymiadis D A and Jones P D 2010 Assessment of maximum possible urbanization influences on land temperature data by comparison of land and marine data around coasts *Atmosphere* **1** 51–61
Emmanuel R and Fernando H 2007 Urban heat islands in humid and arid climates: role of urban form and thermal properties in Colombo, Sri Lanka and Phoenix, USA *Climate Research* **34** 241
He B-J *et al* 2019 An approach to examining performances of cool/hot sources in mitigating/enhancing land surface temperature under different temperature backgrounds based on Landsat 8 image *Sustainable Cities and Society* **44** 416–27
Heinl M, Hammerle A, Tappeiner U and Leitinger G 2015 Determinants of urban–rural land surface temperature differences–a landscape scale perspective *Landscape and Urban Planning* **134** 33–42
Imhoff M L, Zhang P, Wolfe R E and Bounoua L 2010 Remote sensing of the urban heat island effect across biomes in the continental USA *Remote Sens. Environ.* **114** 504–13
Jiménez-Muñoz J C, Sobrino J A, Skoković D, Mattar C and Cristóbal J 2014 Land surface temperature retrieval methods from Landsat-8 thermal infrared sensor data *IEEE Geosci. Remote Sens. Lett.* **11** 1840–3
Middel A, Häb K, Brazel A J, Martin C A and Guhathakurta S 2014 Impact of urban form and design on mid-afternoon microclimate in Phoenix Local Climate Zones *Landscape and Urban Planning* **122** 16–28
Nassar A K, Blackburn G A and Whyatt J D 2016 Dynamics and controls of urban heat sink and island phenomena in a desert city: development of a local climate zone scheme using remotely-sensed inputs *Int. J. Appl. Earth Obs. Geoinf.* **51** 76–90
Nassar A K, Blackburn G A and Whyatt J D 2017 What controls the magnitude of the daytime heat sink in a desert city? *Appl. Geogr.* **80** 1–14
Norton B A, Coutts A M, Livesley S J, Harris R J, Hunter A M and Williams N S 2015 Planning for cooler cities: a framework to prioritise green infrastructure to mitigate high temperatures in urban landscapes *Landscape and Urban Planning* **134** 127–38
Oke T R 1973 City size and the urban heat island *Atmospheric Environment* (1967) **7** 769–79

Onishi A, Cao X, Ito T, Shi F and Imura H 2010 Evaluating the potential for urban heat island mitigation by greening parking lots *Urban Forestry & Urban Greening* **9** 323–332

Peng S S, Piao S, Zeng Z, Ciais P, Zhou L, Li L Z and Zeng H 2014 Afforestation in China cools local land surface temperature *Proceedings of the National Academy of Sciences* **111** 2915–19

Rchid A 2012 The effects of green spaces (palm trees) on the microclimate in arid zones, case study: Ghardaia, Algeria *Energy Procedia* **18** 10–20

Schatz J and Kucharik C J 2014 Seasonality of the urban heat island effect in Madison, Wisconsin *Journal of Applied Meteorology and Climatology* **53** 2371–86

Shen H, Huang L, Zhang L, Wu P and Zeng C 2016 Long-term and fine-scale satellite monitoring of the urban heat island effect by the fusion of multi-temporal and multi-sensor remote sensed data: A 26-year case study of the city of Wuhan in China *Remote Sensing of Environment* **172** 109–25

Song J and Wang Z H 2015 Impacts of mesic and xeric urban vegetation on outdoor thermal comfort and microclimate in Phoenix, AZ *Build. Environ.* **94** 558–68

Spronken-Smith R A and Oke T R 1998 The thermal regime of urban parks in two cities with different summer climates *Int. J. Remote Sens.* **19** 20852104

Verdonck M L, Demuzere M, Bechtel B, Beck C, Brousse O, Droste A and Van Coillie F 2019 The human influence experiment (part 2): guidelines for improved mapping of local climate zones using a supervised classification *Urban Science* **3** 27

Wang Z H, Zhao X, Yang J and Song J 2016 Cooling and energy saving potentials of shade trees and urban lawns in a desert city *Appl. Energy* **161** 437–44

Zhou D, Xiao J, Bonafoni S, Berger C, Deilami K, Zhou Y and Sobrino J 2019 Satellite remote sensing of surface urban heat islands: progress, challenges, and perspectives *Remote Sensing* **11** 48

Zhou D, Zhao S, Liu S, Zhang L and Zhu C 2014 Surface urban heat island in China's 32 major cities: spatial patterns and drivers *Remote Sens. Environ.* **152** 51–61